PAPER

NJC www.rsc.org/njc

Selective assembly of specifically charged proteins on an electrochemically switched surface

Li Mu, Ying Liu, Song Zhang, Baohong Liu and Jilie Kong*

Department of Chemistry, Fudan University, Shanghai, 200433, P. R. China. E-mail: jlkong@fudan.edu.cn; Fax: +86-21-65641740; Tel: +86-21-65642138

Received (in Montpellier, France) 12th July 2004, Accepted 7th March 2005
First published as an Advance Article on the web 5th May 2005

A low-density self-assembled monolayer (LD-SAM) surface was generated *via* covalent bonding between Au and the inclusion complex, cyclodextrin (CD) encapsulated 16-mercaptohexadecanoic acid, followed by the dissociation of CD. The resulted LD-SAM was characterized by cyclic voltammetry, QCM and MALDI-TOF-MS measurements. Electric potential triggered reversible switching property of the LD-SAM was observed by contact angle measurements. The selective assembly of charged proteins, avidin and streptavidin, on the LD-SAM surface, which was carried out under different applied potentials, was investigated by QCM measurements and fluorescence spectrometry.

1. Introduction

The design of a surface with controllable properties is attractive and interesting for its potential applications in controlled molecular assembly,[1] designed wettability alteration[2] and programmed adsorption and release of proteins[3] or cells.[4] Various approaches have been applied to design diverse reversible surfaces, involving photon or charge driven,[5,6] pH or temperature induced,[7,8] and chemically derived or electrochemical modulation.[9,10]

The self-assembled monolayer (SAM) methodology is widely used for designing functionalized surfaces because of its convenience, versatility and ability to introduce various functional groups onto the surface. In the work of Lahann, *et al.*,[10] the preparation of low-density self-assembled monolayers (LD-SAM) is considered to be a key step to ensure the bending of alkanethiol. The mentioned work involves assembling synthetic *capped* alkanelthiolates on a gold surface, followed by disassociating the *cap*, that is the bulky globular groups, to create the LD-SAM. The thus-prepared functional surface is predicted to have potential applications in the dynamic regulation of macroscopic properties, such as biocompatibility. This has been our inspiration to expand it to protein assembly on LD-SAM, described briefly in our preliminary communication.[11]

Instead of using a bulky globular group that is difficult to design and synthesize to *cap* the alkanelthiolates, we use cyclodextrins (CDs) to *wrap* alkanethiol molecules in order to control the density of the SAM on the gold surface. CDs are oligomers with six (α-CD), seven (β-CD), or eight (γ-CD) glucose units. They are commonly employed to form inclusion complexes with various organic molecules because of the hydrophobic and hydrophilic properties of its inner and outer parts, respectively.[12] The inclusion complexes between 16-mercaptohexadecanoic acid (MHA) and α-, β- or γ-CD[6c,12] (abbreviated as *n*-CD-MHA, n = α, β and γ, to represent the inclusion complexes derived from α-, β- and γ-CD in turn) act as the space-filling groups in *n*-SAM (n = α, β and γ represent the SAM derived from α-, β- and γ-CD in turn). Then, removing CD *via* solvent effects creates the *n*-LD-SAM (n = α, β and γ represent the LD-SAMs derived from α-, β- and γ-CD in turn).

The MHA molecules of the *n*-LD-SAMs undergo conformational transitions between "bent" and "straight" states when different potentials are applied to the *n*-LD-SAMs. Thus, controlled protein assembly at pH 7.2 was achieved on the *n*-LD-SAMs by the potential-driven adsorption of two kinds of fluorescent-labelled proteins that have different isoelectric points (IP) and thus can be specifically charged.

In order to confirm our expectations, control experiments have also been carried out on bare and MHA-modified gold surfaces (the latter abbreviated as HD-SAM because of its high density). Since the molecules on the HD-SAM are compactly packed, their conformation will not change even when an external stimulation is applied to them.[13]

2. Experimental

2.1 Materials and reagents

Solvents such as absolute ethanol and deuterium oxide were used as purchased. All the others were analytical reagents. Highly purified water (>18 MΩ) was used for all experiments. For the synthesis of the *n*-CD-MHA, 16-mercaptohexadecanoic acid [$SHCH_2(CH_2)_{14}COOH$, MHA, Aldrich; 99%], α-CD (Fluka Chemical), β-CD (Shanghai Chemical Reagents Co.), and γ-CD (Fluka Chemical) were also used as received. Two kinds of fluorescent-labelled proteins, avidin (A-821, IP ~10.5, Sigma) and streptavidin (IP ~6.3, A-11230, Sigma) were used for the controlled protein adsorption experiments.

2.2 Instrumentation

The high-resolution ^1H NMR spectra were recorded on a Bruker 500 MHz spectrometer at room temperature. CDs (α-, β- and γ-CD) and *n*-MHA were dissolved in deuterium oxide.

The cyclic voltammetry (CV) measurements were performed on a CHI-1030 Electrochemical Workstation (Shanghai Chenhua Co.) with three electrodes: Hg/Hg_2Cl_2 as the reference electrode (internal solution: saturated KCl aqueous solution), a Pt wire electrode as the counter electrode and the SAM modified gold electrode (or bare gold electrode) as the working electrode. It was polished with emery paper, followed by alumina on a soft polishing cloth (Shanghai Chenhua Co.). All solutions were freshly prepared and were purged with nitrogen for 15 min before measurements.

DOI: 10.1039/b410610e

QCM measurements were carried out with QCM oscillators (gold disk area $A = 0.2043\ cm^2$, CH Instrument) on a CHI-400 Electrochemical Crystal Microbalance (CH Instrument, Austin, TX, USA).

MALDI-TOF-MS measurements were performed on a 4700 Proteomics Analyzer (ABI Instrumental Co.) with a matrix solution containing α-CHCA (5 mg mL^{-1}) in 50% acetonitrile solution and 0.1% TFA (trifluoroacetic acid).

Contact angle measurements were performed on a Phoenix-300 (SEO Co. Ltd, Korea).

The fluorescence (FL) spectra were recorded with an SM-300 CCD Fluorescent Spectrometer (CVI Spectral Co. Ltd, Putnam, CT, USA). The excitation wavelength was 499 (365) nm and the detection wavelength was set at 508 (460) nm for avidin (streptavidin).

2.3 Sample preparation and characterization

2.3.1 Synthesis and characterization of *n*-CD-MHA. MHA (20 mg) was added to an aqueous solution of 270 mg α-CD (315 mg for β-CD and 360 mg for γ-CD) in 20 mL purified water with a molar ratio of 1 : 4 (excess CD was used in order to ensure that the majority of MHA in solution was bound by CD molecules). The resulting mixture was kept in an oil bath (313.1 ± 0.1 K) with stirring for more than 48 h, and then cooled to room temperature and filtered. The product (synthesized in deuterium oxide) was analyzed by ^{1}H NMR.

2.3.2 Assembly of *n*-CD-MHA on Au surface to generate *n*-SAM and removal of CD to creat *n*-LD-SAM. The resulting *n*-CD-MHA was used as a loading solution to assemble monolayers. The gold electrode, after being cleaned thoroughly (sonication in absolute ethanol and then in water),[13] was electrocycled between 0.6 V and −0.2 V (*vs.* SCE) in 2.5 mM $K_3Fe(CN)_6/K_4Fe(CN)_6$ until a reproducible voltammogram was obtained. The gold electrode (or the QCM oscillators with gold disk, also cleaned thoroughly) was immediately immersed in the loading solution for 16 h at 277.1 K. It was taken out from the solution, rinsed vigorously with purified water and blown dry with pure nitrogen prior to use.

Different organic solvents (including DMSO, *n*-butanol, ethanol, *etc.*) were tested for the dissociation of the inclusion complexes.[14] The dissociation was investigated with cyclic voltammetry. The CDs were found to be efficiently removed by absolute ethanol by continuous rinsing for more than 5 min, followed by immersing in absolute ethanol for another 25 min to ensure that the CDs were completely removed. The resulting *n*-LD-SAMs were gently blown dry with nitrogen for further experiments.

The assembly and removal of α-, β- and γ-CD was investigated by QCM, CV, and MALDI-TOF-MS.

During the washing process, CV and QCM measurements were performed on the bare gold electrode (or the QCM oscillator) and the *n*-SAM modified gold electrodes (or the QCM oscillators) before and after their being rinsed in absolute ethanol for 0, 1 and 5 min (recorded at 0, 15, 30, 45 s, 1, 2, 3, 5, 10, 15, 20, 25, 30 min in QCM measurements). Control experiments were also carried out on the MHA-modifed gold electrode (or the QCM oscillator) in order to find out whether absolute ethanol can destroy the Au–S bond.

In the MS measurements, ionization was performed with a Nd : YAG laser with an emission wavelength of 355 nm. It produced pulses of 3 to 7 ns duration. The laser repetition rate was 200 Hz. The acceleration voltage was kept at 6 kV. Positive ions were detected on a time-of-flight mass detector in the reflector mode. Two microliters of the matrix solution was added directly onto the QCM oscillator modified with *n*-SAM or *n*-LD-SAM. After being dried in air, the oscillator was attached directly onto a MALDI sample plate and loaded into the 4700 Proteomics Analyzer for the measurements.

2.3.3 Contact angle measurement of *n*-SAM. Contact angle measurements were performed on a Phoenix-300 (SEO Co. Ltd, Korea) with MHA-SAM-modified oscillators as working electrode coupled with a fine silver wire ($\phi = 0.1$ mm) and a platinum wire ($\phi = 0.2$ mm) employed as the quasi-reference electrode and counter electrode; *in situ* electrochemical modulations was performed on a CHI-600 Electrochemical Workstation. The applied potential were controlled at the values calibrated by SCE. A 100 μL droplet of PBS buffer (pH = 7.4) was used as electrolyte and the image of the droplet was taken to measure the contact angle at the different applied potentials. A gold slide (1 cm × 1 cm), on which the same HD-SAM was prepared, was also used as the working electrode to measure the contact angle to compare with the results obtained on the Au oscillator.

2.3.4 Potential-controlled protein assembly on the *n*-LD-SAM. The prepared *n*-LD-SAMs were immersed in PBS buffer (pH = 7.4) containing 1.0 mg L^{-1} avidin or 0.5 mg L^{-1} streptavidin at an applied potential of −0.3 V [denoted as (−)], +0.3 V [denoted as (+)] (both *vs.* SCE, the applied potential was chosen above the lower limit for transitions and within the "window of stability")[15] and at open circuit [denoted as (0)] for 30 min. Then the *n*-LD-SAMs were then thoroughly rinsed with purified water and blown dry with pure nitrogen for further QCM and FL measurements.

3. Results and discussion

3.1 Characterization of the prepared *n*-CD-MHA

The formation of *n*-CD-MHA was proved by ^{1}H NMR spectra. In solution, ^{1}H NMR is known to be a good method to confirm the existence of an inclusion complex.[16] As shown in Table 1 and Fig. 1, there is a significant upfield shift for the internal H-3 and H-5 protons (Scheme 1), which are more sensitive to the complexation effect than the H-1, H-2, H-4 protons located on the outside of the host cavity. The signals from H-6a and H-6b were also shifted upfield but less than those for the H-3 and H-5 protons. The shifts of these protons to higher field was accompanied by increasing shielding during complex formation of *n*-CD-MHA, as a result of the release of water molecules from the cavity, which are replaced by the apolar alkyl chain of the MHA guest.[16]

3.2 Evidence for the formation of *n*-LD-SAM

3.2.1 Cyclic voltammetic results. Cyclic voltammetric sweeping in redox couple-containing buffer directly provides the surface properties of bare or functionalized electrodes. As shown in Fig. 2(A), the peak current (i_p) for the bare gold electrode is the highest, while for the β-SAM modified electrode it is the lowest, which is because the β-CD-MHA SAM is

Table 1 Characterization of *n*-CD-SAM with ^{1}H NMR[a]

Sample	H-1	H-2	H-3	H-4	H-5	H-6
α-CD	4.95	3.54	3.89	3.48	3.74	3.76
α-CD-MHA	4.95	3.54	3.83	3.48	3.69	3.76
β-CD	4.94	3.54	3.87	3.50	3.73	3.75
β-CD-MHA	4.94	3.52	3.71	3.49	3.59	3.65
γ-CD	5.01	3.56	3.85	3.51	3.75	3.77
γ-CD-MHA	5.01	3.56	3.79	3.50	3.68	3.76

[a] All the data were recorded on a Bruker 500 MHz spectrometer at room temperature and all the samples were dissolved in deuterium oxide.

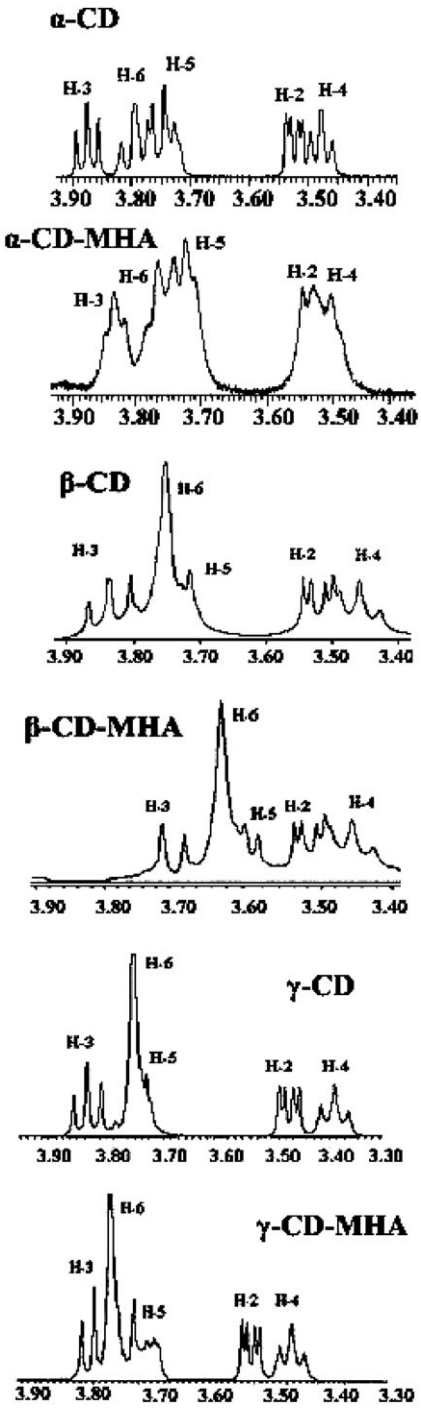

Fig. 1 ^{1}H NMR spectra of α-, β-, γ-CD and *n*-CD-MHA. All the data were recorded on a Bruker 500 MHz spectrometer at room temperature and all the samples were dissolved in deuterium oxide.

insulating to a certain extent. Along with washing the β-SAM modified electrode with absolute ethanol, which removes the CDs, the conductive gold surface is gradually exposed to redox processes in solution. As a result, the redox peak in the *i–V*

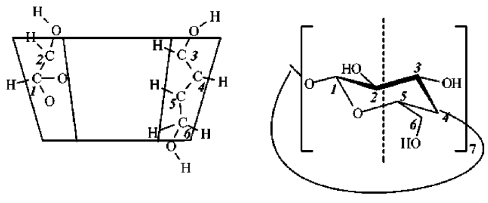

Scheme 1 Structure for β-CD and the inside/outside orientation of the protons.[16]

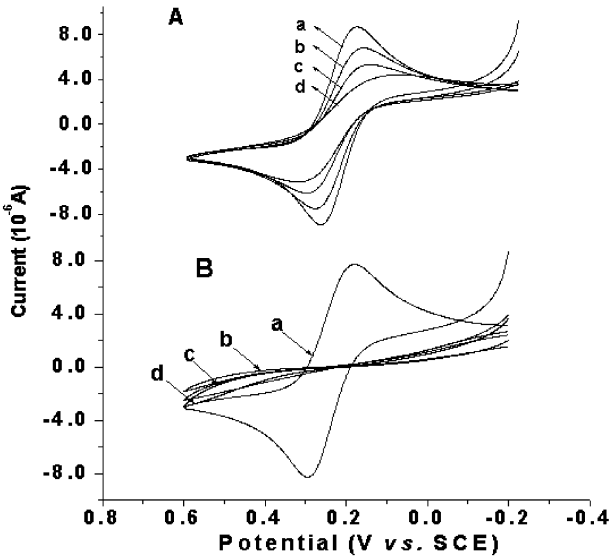

Fig. 2 Cyclic voltammograms of (a) bare Au (in both A and B) and (A) β-CD-SAM and (B) HD-SAM modified electrodes rinsed in absolute ethanol for (b) 5 , (c) 1 and (d) 0 min. Scan rate: 10 mV s^{-1};, electrolyte is a solution containing $K_3Fe(CN)_6/K_4Fe(CN)_6$ (2.5 mmol L^{-1}) and KCl (100 mmol L^{-1}). The electrode was gently blown dry with pure nitrogen before every measurement.

curve develops much higher. These phenomena confirm the assembly of β-SAM and the removal of β-CD.

We can also see from Fig. 2(A) that the i_p of the *i–V* curve for the so-prepared β-LD-SAM is lower than that for bare gold, since parts of the electroactive area of the β-LD-SAM modified electrode are still covered by the insulating MHA molecules.

Control experiments were carried out with HD-SAM modified gold electrode; the results are shown in Fig. 2(B). The assembly of MHA molecules onto the electrode resulted in a distinct decrease in i_p; along with washing the modified electrode with absolute ethanol, no similar increase in i_p could be observed as in Fig. 2(A). So we can conclude that MHA molecules pack compactly on the surface, insulating it, and its surface coverage is larger than that on the β-SAM modified electrode (see Table 2 below). It is more important to conclude from the QCM data that the Au–S bond is stable, even to washing by absolute ethanol, while CDs are readily removed, as proved by the MALDI-TOF-MS and QCM results.

We only list the CV results of β-SAM here, CV measurement results for α- and γ-SAM are basically similar.

3.2.2 QCM measurements of the *n*-SAM and the *n*-LD-SAM. QCM measurement data definitely reflect the quantitative removal of α-, β or γ-CD from the surface. Table 2 shows the frequency shift (Δf), the corresponding mass change (ΔM)

Table 2 Characterization of *n*-LD-SAM with QCM[a]

Type of SAM	Δf_1[b]/ Hz	ΔM_1[b]/ nmol cm^{-2}	Δf_2[c]/ Hz	Γ_2[c]/ nmol cm^{-2}	θ[c] (%)
α-SAM	94.2	−0.616	−104.4	2.08	61.2
β-SAM	76.7	−0.430	−55.3	1.54	45.3
γ-SAM	54.1	−2.66	−30.6	0.99	29.2

[a] All data were the average of three measurements with standard deviations of less than 10%. [b] Δf_1 is the frequency shift between the dissociated and undissociated α-, β- or γ-CD; ΔM_1 represents the mass loss for the corresponding *n*-CD calculated from Δf_1. [c] Δf_2 is the frequency shift for the relevant *n*-LD-SAM deduced from Δf_2; θ represents the surface coverage of *n*-LD-SAM calculated from $\theta = \Gamma_2/\Gamma_0 \times 100$, where Γ_0 is the surface concentration for HD-SAM.

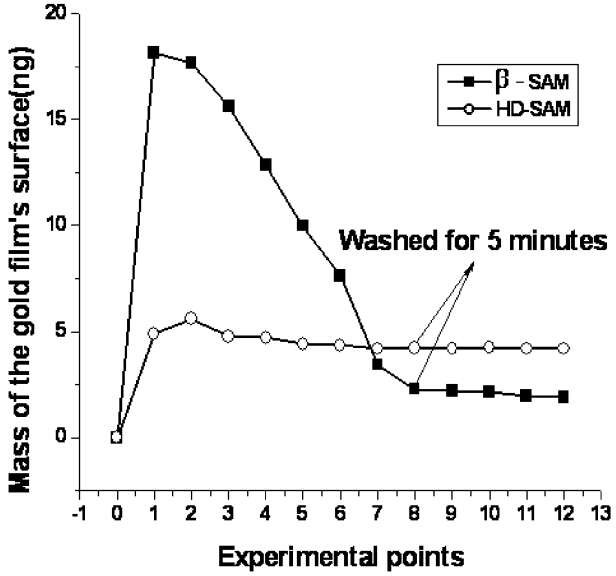

Fig. 3 QCM measurement response for β-SAM (filled squares) and HD-SAM (open circles) modified oscillators during the experimental process. The experimental point 0 represents a bare gold QCM oscillator; points 1 to 12 represent modified oscillators that have been rinsed in absolute ethanol for 0, 15, 30, 45 s, 1, 2, 3, 5, 10, 15, 20 and 30 min. The QCM oscillator was gently blown dry with pure nitrogen before every measurement.

and the calculated surface coverage (θ) for the *n*-LD-SAM, referenced to HD-SAM; it shows an obvious decrease from 100% to 61.2%, 45.3% and 29.2%, respectively, for α-, β- and γ-LD-SAM. This can be reasonably attributed to the removal of CDs from the surface.

In addition, as shown in Fig. 3, the distinct increase of the oscillator surface mass demonstrates the assembly of β-SAM onto the oscillator surface. The subsequent decrease of the mass indicates that β-CD is removed with absolute ethanol; after the oscillator was rinsed in absolute ethanol for 5 min, the mass almost did not change with further washing. This shows that the sought-for β-LD-SAM was prepared within that time.

Control experiments were carried out with an HD-SAM modified oscillator. It showed a much smaller increase of the oscillator surface mass than that of the β-SAM modified oscillator and when washing with absolute ethanol, the mass did not change significantly. These observations confirm the assembly of MHA molecules on the oscillator and the stability of the Au–S bond in absolute ethanol.

We only show the results of the QCM measurements for β-SAM. For α- and γ-SAM, similar results were obtained.

3.2.3 MALDI-TOF-MS measurements of the *n*-SAM and the *n*-LD-SAM. The results of MALDI-TOF-MS measurement also confirmed the removal of α-, β- or γ-CD from *n*-SAM. As shown in Fig. 4, comparing the spectra of each *n*-SAM with its corresponding *n*-LD-SAM, it can be seen that after washing with absolute ethanol, the peaks at 995.2, 1158.2 and 1319.5 (*m*/*z*) disappeared for α-, β- and γ-SAM, respectively. These are the molecular peaks for α-, β-, γ-CD, respectively, with sodium ion.

3.3 Reversible switching properties of *n*-LD-SAM

The electric potential triggered reversible switching properties, such as the switchable wettability, of the *n*-LD-SAM were investigated by contact angle measurements. A remarkable dissimilarity in the contact angles of polar medium on *n*-LD-SAM was observed: the contact angle of buffer (pH = 7.4) on β-SAM was measured to be about 55° for an applied potential E_{appl} = +0.3 V and to be about 22° at E_{appl} = −0.3 V, which

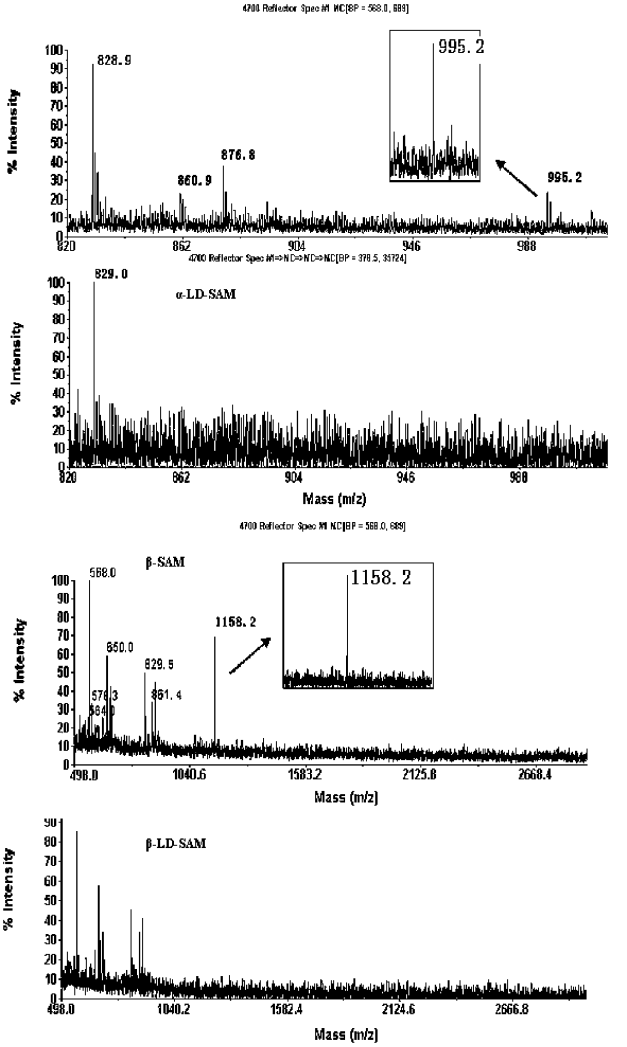

Fig. 4 MALDI-TOF-MS for α-, β- and γ-SAM and α-, β- and γ-LD-SAM. The inserts show the *m*/*z* of the *n*-CDs. Ionization performed with an Nd : YAG laser. Emission wavelength: 355 nm. Pulses duration: 3 to 7 ns. Laser emission rate: 200 Hz. Acceleration voltage: 6 KV. All peaks except for the α-, β- and γ-CD molecular ions arise from the matrix solution.

strongly implies that a surface transition between the hydrophilic (MHA molecules are linear) and hydrophobic (MHA molecules are bent) states occurs. Therefore, the surface charge of the *n*-LD-SAM could be controlled in two ways: one was fully negatively charged and hydrophilic, with the carboxyl-terminated thiol extending straight into the solution at negative applied potential [(−) or *on* state]; the another was neutral and hydrophobic, with the bent chain exposed to the solution, driven by a positive potential [(+) or *off* state]. These two states can be reversibly switched as desired by simply changing the applied potential.

3.4 Controlled protein assembly on the *n*-LD-SAM

After avidin or streptavidin adsorption onto the *n*-LD-SAM, the distinctly opposite assembly behavior of the two proteins at the two controlled potentials was observed from the QCM and FL data (Table 3 and Fig. 5). Fig. 6 shows the relative FL emission intensity and mass for the two assembled proteins at the (0), (+) and (−) states. For example, the emission intensity for the avidin assembled α-LD-SAM at (−) for 30 min is about 4.9 times that at (+). Similarly, the FL emission intensity for avidin modified β- and γ-LD-SAM at (−) for 30 min is about 5.0 and 4.6 times those at (+), respectively. These values are basically consistent with the calculated protein loadings from the measured QCM data given in Table 3.

Table 3 Absolute mass change and FL emission intensity for the protein modified *n*-LD-SAMs

SAM	Protein Surface potential	Avidin (+)	Avidin (0)	Avidin (−)	Streptavidin (+)	Streptavidin (0)	Streptavidin (−)
α-LD-SAM	QCM/ng cm^{-2}	122.2	402.2	664.3	316.3	219.5	186.4
	FL	124.7	460.6	810.0	78.1	63.0	45.7
β-LD-SAM	QCM/ng cm^{-2}	91.6	268.5	465.8	194.7	159.7	120.3
	FL	92.6	324.9	615.1	50.9	42.6	35.1
γ-LD-SAM	QCM/ng cm^{-2}	68.1	148.9	372.9	108.2	71.3	46.5
	FL	87.1	204.8	397.6	41.6	34.0	30.0

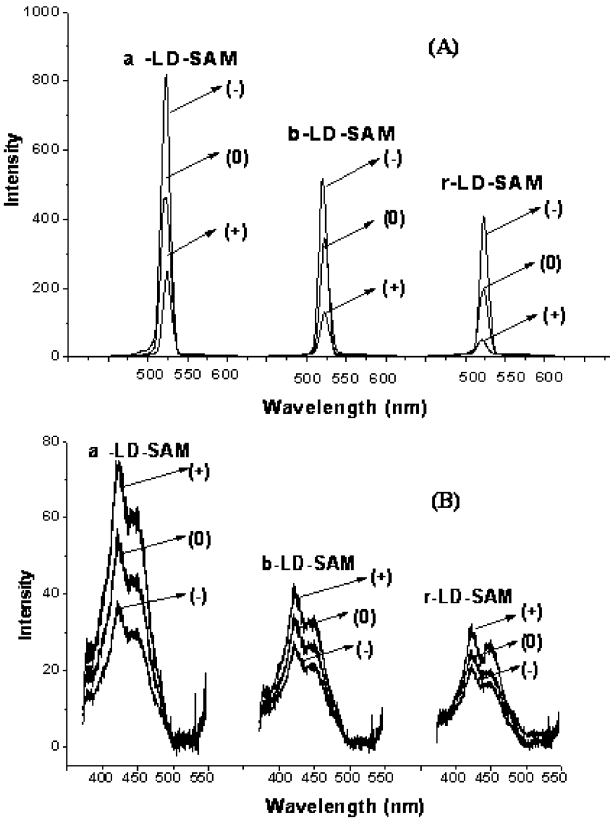

Fig. 5 FL emission spectra for (A) avidin and (B) streptavidin modified *n*-LD-SAM at controlled applied potentials [(−), (+) and (0)]. The detection wavelength was set at 508 nm and the excitation wavelength was 499 nm for avidin; for streptavidin, the detection wavelength was 460 nm and the excitation wavelength was 365 nm.

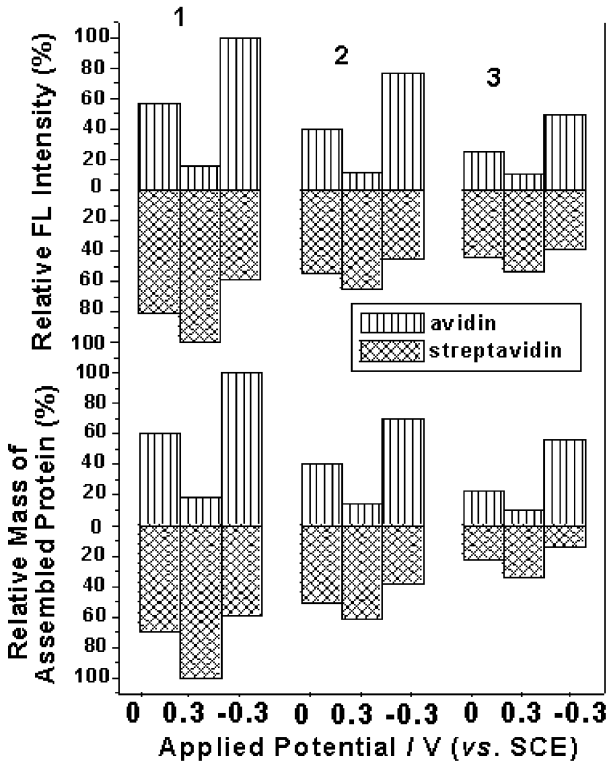

Fig. 6 Avidin and streptavidin modified *n*-LD-SAM measured by FL spectrometry and QCM. The 1, 2 and 3 above the bars represent the α-, β- and γ-LD-SAM, respectively. All FL intensity and mass date are the average values of three measurements and normalized to the maximum value of each measurement. 0 on the *x* axis represents the surface state at open circuit.

Thus, the switchable surface shows a unique feature of controlled assembly for the positively charged avidin, while for streptavidin assembly on *n*-LD-SAM, weaker emission intensities were observed at (−) compared with those at (0) and (+), corresponding to less protein attachment. On the contrary, with the positive applied potential, protein loadings were about 1.7, 1.5 and 1.4 times those found with a negative applied potential for streptavidin modified α-, β- and γ-LD-SAM, respectively. So, the opposite assembly behavior for avidin at the two charge states strongly suggests that the surface transition occurs upon switching the applied potentials, affecting both proteins. The dissimilar behavior of these two charged proteins is believed to be due to their different isoelectric points (IP), that is, the IP for avidin is 10.5 and that for streptavidin is 6.3, which means avidin is positively charged and streptavidin is slightly negatively charged at neutral pH. Thus, specifically charged proteins can be selectively attached on the electrochemically controlled surface.

3.5 Control experiments

In order to confirm that the opposite assembly behaviour of avidin and streptavidin at the different applied potentials is due to the conformational transition of the *n*-LD-SAM at the different electronic potentials, two control experiments were performed. The amount of protein assembled on a bare gold surface, resulting solely from the electrostatic adsorption or repulsion, was about only 5–10% of that on *n*-LD-SAM when the same potential was applied, which suggested that it was the

Table 4 Comparison of protein adsorption for *n*-LD-SAM and HD-SAM[a]

SAM	Protein Surface potential	Avidin (+)	Avidin (0)	Avidin (−)	Streptavidin (+)	Streptavidin (0)	Streptavidin (−)
A-LD-SAM	Δf (Hz)	19.2	63.2	104.3	49.7	34.5	29.3
	Γ_1	122.2	402.2	664.3	316.3	219.5	186.4
HD-SAM	Δf_0(Hz)	135.3	137.1	140.7	75.0	71.7	70.4
	Γ_{11}	861.4	872.7	895.8	477.3	456.2	448.1

[a] All data are the average of three measurements with standard deviations of less than 10%. Δf and Δf_0 are the frequency shifts after protein adsorption. Γ_1 and Γ_{11} (in ng cm^{-2}) are the corresponding surface concentrations of the proteins.

conformation of *n*-LD-SAM, instead of the static electricity on bare gold,[17] that dominated the protein attachment.

Furthermore, Table 4 shows that the applied potential has no effect on the protein adsorption onto HD-SAM, while it has a significant effect for α-LD-SAM. So we can conclude that it is the potential-controlled chain bending, but not the protonation of the terminal carboxylic acid groups, that contributes to the selective protein adsorption.

4. Conclusions

This work demonstrated the formation of *n*-LD-SAM by assembling pre-formed inclusion complexes, α-, β- and γ-CD wrapped MHA, on gold surfaces, followed by unwrapping of the CDs from the anchored MHA molecules. The thus-prepared *n*-LD-SAM were proved to be electrochemically induced reversible switching surfaces. They exhibit a conformational transition between "bent" and "linear" states, which represent the ionized carboxyl groups or the alkyl chains of MHA facing outside, respectively, at different applied potentials. As a result, the *n*-LD-SAM can exhibit either hydrophobic or hydrophilic properties as desired. Thus, potential-controlled selective protein adsorption of two fluorescent-labelled proteins on the *n*-LD-SAM was successfully achieved.

These results are a successful example of how to design a desired surface and on how to control the assembly of specific kinds of proteins. We believe that it might lead to versatile applications, for example, controlled protein adsorption/release in an as-functionalized capillary or microfluidic channel, or design of intelligent protein chips. We are continuing our work to achieve the same result in a micro-channel on a chip.

Acknowledgements

This work was supported by NSFC (20335040), 973 (2001CB5102), 863 (2002AA63918), SKLEAC and Fudan graduate innovation funds.

References

1 (*a*) T. P. Russell, *Science*, 2002, **297**, 964; (*b*) C. M. Stafford, A. Y. Fadeev, T. P. Russell and T. J. McCarthy, *Langmuir*, 2001, **17**, 6547; (*c*) H. Hiramatsu and F. E. Osterloh, *Langmuir*, 2003, **19**, 7003.
2 Z. Q. Lin, T. Kerle, T. P. Russell, E. Schaffer and U. Steiner, *Macromolecules*, 2002, **35**, 6255.
3 D. L. Huber, R. P. Manginell, M. A. Samara, B. I. Kim and B. C. Bunker, *Science*, 2003, **301**, 352.
4 X. Y. Jiang, R. Ferrigno, M. Mrksich and G. M. Whitesides, *J. Am. Chem. Soc.*, 2003, **125**, 2366.
5 (*a*) S. Abbott, J. Ralston, G. Reynolds and R. Hayes, *Langmuir*, 1999, **15**, 8923; (*b*) K. Ichimura, S. K. Oh and M. Nakagawa, *Science*, 2000, **288**, 1624; (*c*) S. K. Oh, M. Nakagawa and K. Ichimura, *J. Mater. Chem.*, 2002, **12**, 2262; (*d*) I. Willner, A. Doron, E. Katz, S. Levi and A. F. Frank, *Langmuir*, 1996, **12**, 946.
6 (*a*) J. Weissmuller, R. N. Viswanath, D. Kramer, P. Zimmer, R. Wurschum and H. Gleiter, *Science*, 2003, **300**, 312; (*b*) Y. Y. Luk and N. L. Abbott, *Science*, 2003, **301**, 623; (*c*) S. Chen, L. Liu, J. Zhou and S. Jiang, *Langmuir*, 2003, **19**, 2859; (*d*) I. Willner, A. Doron, E. Katz, S. Levi and A. F. Frank, *Langmuir*, 1996, **12**, 946.
7 J. R. Matthews, D. Tuncel, R. M. J. Jacobs, C. D. Bain and H. L. Anderson, *J. Am. Chem. Soc.*, 2003, **125**, 6428.
8 (*a*) M. Arotcarena, B. Heise, S. Ishaya and A. Laschewsky, *J. Am. Chem. Soc.*, 2003, **124**, 3787; (*b*) G. B. Crevoisier, P. Fabre, J. M. Corpart and L. Leibler, *Science*, 1999, **285**, 1246.
9 (*a*) G. M. Whitesides and B. Grzybowski, *Science*, 2002, **295**, 2418; (*b*) J. Lahiri, L. Isaacs, B. Grzybowski, J. D. Carbeck and G. M. Whitesides, *Langmuir*, 1999, **15**, 7186; (*c*) M. Mrksich, C. S. Chen, Y. N. Xia, L. E. Dike, D. E. Ingber and G. M. Whitesides, *Proc. Natl. Acad. Sci. USA*, 1996, **93**, 10775.
10 (*a*) J. Lahann, S. Mitragotri, N. T. Tran, H. Kaido, J. Sundaram, S. I. Choi, S. Hoffer, A. G. Somorjai and R. Langer, *Science*, 2003, **299**, 371; (*b*) M. X. Wang, B. A. Kharitonov, T. Katz and I. Willner, *Chem. Commun.*, 2003, **13**, 1542.
11 Y. Liu, L. Mu, B. H. Liu, S. Zhang, P. Y. Yang and J. L. Kong, *Chem. Commun.*, 2004, **10**, 1194.
12 H. Ikeda, M. Nakamura, N. Ise, N. Oguma, A. Nakamura, T. Ikeda, F. Toda and A. Ueno, *J. Am. Chem. Soc.*, 1996, **118**, 10980.
13 Juchao Yan and Shaojun Dong, *J. Electroanal. Chem.*, 1997, **440**, 229.
14 (*a*) K. A. Connors and S. Sun, *J. Am. Chem. Soc.*, 1971, **93**, 7239; (*b*) J. Pitha and T. Hoshino, *Int. J. Pharm.*, 1992, **80**, 243.
15 E. Boubour and B. R. Lennox, *J. Phys. Chem. B*, 2000, **104**, 9004.
16 T. Bojinova, Y. Coppel, L. N. Viguerie, A. Milus, I. Rico-Lattes and A. Lattes, *Langmuir*, 2003, **19**, 5233.
17 Experiments run at (0) gave the protein loading adsorbed on the surface when no external voltage was applied; these values were employed as the references in Fig. 6 to distinguish the protein assembly on freely existing (0) or potential-controlled (+) or (−) surfaces.